that *P. frontalis* spends 2 or 3 years in the hyporheic habitat before emerging. The *Isocapnia* species have at least a 2-year life cycle (*8*). Chironomids, young mayflies of the genera *Ammeletus* and *Rhithrogena*, early instar capniid stone flies, larval and adult riffle beetles, water mites, and several leeches were also taken from the galleries. Hauls made in the pump reservoir with a plankton net revealed that periphytic rhithron algae (mostly diatoms) and riverine detritus were passed through galleries abundantly. Except for *P. frontalis*, the *Isocapnia* species, and the leeches, all these organisms are common in the rhithron habitat of the Tobacco River. Obviously, a variety of potential food items either crawl or are carried passively by waters percolating downward and laterally to resident consumers living deep in the substrata. Interstices in floodplain gravel are apparently wide enough to allow fairly large invertebrates to move efficiently. While we can only demonstrate that four species, all large stone flies, are permanent residents of subterranean waters in the floodplains of the Tobacco River, it is clear that a diverse community exists deep in substrata. Many of the hyporheic residents are small benthic insects recruited from the surface of the river bottom and may move back and forth from channel to hyporheic habitats.

We have shown that the hyporheic community of the Tobacco River extends to a depth of at least 4.2 m and up to 50 m laterally from the river channel. Since no adjacent wells or infiltration galleries were available to facilitate sampling, we could not specifically determine the dimensions of hyporheic development of the larger Flathead River. Considering the tremendous emergence of *P. frontalis* and *Isocapnia* species and more extensive deposits of floodplain gravel, the hyporheic area of the Flathead probably extends several hundred meters from the channel and to considerable depth. It is likely that any stream or river with a similar hydrogeology will exhibit extensive hyporheic areas. We emphasize that deep hyporheic habitats may exist only in streams in which the channel and adjacent substrata are composed of loosely compacted floodplain gravels (*9*). The macrobenthic habitat in such streams is three-dimensional (Fig. 2). A channel habitat supports a diverse fauna in a mozaic of microhabitats which develop as a consequence of natural fluvial processes. The hyporheic area is inhabited by a more limited variety of organisms utilizing food carried by both active and passive transportation in waters moving vertically and laterally from the stream channel. For species that must emerge to reproduce, there is also a terrestrial habitat with associated ecological consequences.

In rubble-bottom rivers with extensive hyporheic areas the problem of quantifying production becomes extremely perplexing. Our observation that macrobenthic species occurring very abundantly as adults along the shoreline may be impossible to find by channel sampling indicates the possible magnitude of hyporheic production. Concerted effort and sampling ingenuity by stream limnologists will be required to adequately evaluate the function of the hyporheic community in the stream ecosystem.

Sanitary engineers should consider the possibility of encountering hyporheic organisms when they plan the construction of infiltration galleries. While the macroinvertebrates we observed are not at all a health hazard, Eureka residents certainly considered them a nuisance.

JACK A. STANFORD*
University of Montana Biological Station, Bigfork 59911

ARDEN R. GAUFIN
Department of Biology, University of Utah, Salt Lake City 84112

References and Notes

1. K. W. Cummins and G. H. Lauff, *Hydrobiologia* **34**, 145 (1969).
2. H. B. N. Hynes, *Ecology of Running Waters* (Univ. of Toronto Press, Toronto, 1970).
3. E. Angelier, *Arch. Zool. Exp. Gen.* **90**, 37 (1953); M. J. Coleman and H. B. N. Hynes, *Limnol. Oceanogr.* **15**, 31 (1970).
4. T. Orghidan, *Arch. Hydrobiol.* **55**, 392 (1959).
5. J. Schwoerbel, *ibid.* **25** (Suppl.), 182 (1961).
6. J. A. Stanford and E. B. Reed, *Water Resour. Bull.*, in press.
7. Stone fly naiads taken from the galleries alive appear to be quite tolerant of low concentrations of dissolved oxygen. We have held 20 to 30 naiads in sealed 10-dram (~ 35-cm^3) vials for 10 hours at room temperature with no mortality.
8. The nymphs of these species have not yet been described taxonomically. We have associated nymphs with adults and are now certain of identifications. Our *Isocapnia* growth data are difficult to interpret because of the peculiar occurrence of dwarf males of *I. missouri* and *I. crinita*.
9. Plecopterans like or closely related to the hyporheic forms we encountered are rather uncommonly collected in North America, but the records we are familiar with strongly suggest that these stone flies reside in hyporheic habitats of other streams. W. Ricker has examined *Isocapnia* larvae from a water supply system for the small city of Banff, Alberta, Canada; source wells are located in floodplain gravel near Spray River. Numerous *I. integra* emerge from the river in the spring. Ricker also reported collecting *P. frontalis* naiads from wells 6 to 15 m deep in gravel deposits a few hundred meters from the Nanamio River, British Columbia, Canada (personal communication). A single vial containing three *Paraperla* sp. nymphs collected from a well at Chitina, Alaska, in 1934 was found by R. Baumann in the Plecoptera collection of the Smithsonian Institution, Washington, D.C. D. Potter has shown us specimens of a closely related species, *Kathroperla perdita* Banks, from a drilled well in W. T. Galliver Provincial Park, Alberta, Canada. These nymphs could have come from subterranean waters from 3 to 16 m below ground level. Adults apparently emerge from spring creeks nearby. Other collections of *Paraperla* and *Isocapnia* nymphs are rare and primarily limited to mature naiads ready to emerge. Adults, however, have been found along streams and rivers throughout the Rocky Mountains. In the few locations where these stone flies have been collected abundantly, substrate conditions were similar to those described in this report. It is likely that nymphs resided in hyporheic areas. The precise combination of substrata required for extensive hyporheic development is also comparatively uncommon. Often stream substrata are tightly compacted by deposition of fine sediments filling interstices. The result is reduced percolation of river water through the substrata, and a poorly oxygenated or even anaerobic layer may be present a few centimeters below the surface of the river bottom, precluding hyporheic colonization. However, many of the larger streams and rivers of the Pacific Northwest and Alaska are quite similar to the Tobacco and Flathead rivers, and we would expect to find well-developed hyporheic communities in them.
10. We thank A. Sheldon, G. W. Prescott, W. Ricker, R. Baumann, J. Tibbs, D. Potter, D. Carver, and W. Miller for their help.
* Present address: Department of Biological Sciences, North Texas State Univ., Denton 76203.

22 April 1974

Comet Kohoutek: Ultraviolet Images and Spectrograms

Abstract. *Emissions of atomic oxygen (1304 angstroms), atomic carbon (1657 angstroms), and atomic hydrogen (1216 angstroms) from Comet Kohoutek were observed with ultraviolet cameras carried on a sounding rocket on 8 January 1974. Analysis of the Lyman alpha halo at 1216 angstroms gave an atomic hydrogen production rate of* 4.5×10^{29} *atoms per second.*

On 8 January 1974 at 0140 U.T. we flew a group of ultraviolet cameras and photometers on an Aerobee rocket over White Sands, New Mexico, to observe Comet Kohoutek. At the time of the observations the comet was 0.43 A.U. from the sun and twice that far from the earth; the sun-comet-earth angle was close to 90°. Among the instruments carried were three ultraviolet-sensitive electronographic cameras, of the type used in the Lunar Surface Ultraviolet Camera/Spectrograph on the Apollo 16 mission to photograph (among other things) the hydrogen corona surrounding the earth (*1*). One

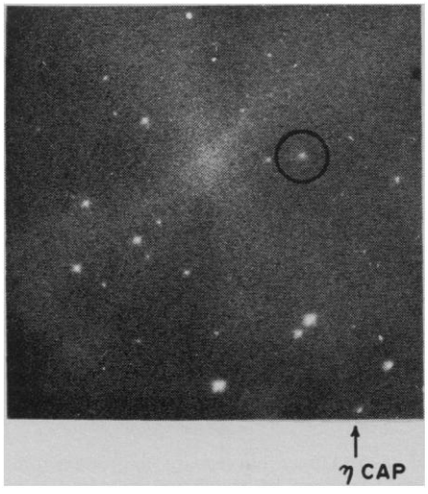

Fig. 1. Image of a region 10° square near Comet Kohoutek in the wavelength range 1250 to 1900 Å (100-second exposure). The comet (circled) is comparable in ultraviolet brightness to the 5th magnitude star of spectral class A4 Eta Capricorni (η Cap) at the lower right. Most of the radiation is due to the atomic oxygen line at 1304 Å and the atomic carbon line at 1657 Å.

camera was sensitive to the wavelength range 1100 to 1500 Å, and two others were sensitive to the range 1250 to 1900 Å. One of the latter was pointed at an objective grating to obtain spectra of the comet. All three cameras produced good data, which we present in preliminary form here.

The electronographic cameras incorporate $f/1$ Schmidt optical systems with 75-mm focal lengths. The spectral responses are determined by the choice of photocathode and corrector plate materials (KBr and LiF for the short-wavelength camera, and CsI and CaF_2 for the others). The resolution of the cameras is 2 arc minutes, and they have 20° fields of view. Exposures from 0.75 to 15 seconds were used with the short-wavelength camera; no longer exposures were used because of background due to the intense Lyman α geocoronal glow at 1216 Å. Exposures of up to 100 seconds were used with the longer-wavelength cameras, as the only airglow emissions of any consequence in this passband were relatively faint emissions of atomic oxygen at 1304 and 1356 Å. The airglow brightnesses were measured with accurately calibrated photometers and compared with the diffuse background on the film in order to provide in-flight calibrations of the camera sensitivities. In addition, we obtained images and spectra of a star field in Perseus which will help to refine the photometric accuracy further. The cameras were fixed in the rocket, and the entire rocket was pointed in the general direction of the comet by cold gas jets, according to a program based on an inertial reference system. It was then stabilized to 1 arc min/min by rate-integrating gyros. All exposures were made above an altitude of 150 km.

A 100-second exposure with the direct imaging camera (1250 to 1900 Å) produced a circular image about 10 arc minutes (4×10^5 km) across (Fig. 1). The same exposure with the spectrograph revealed that the emissions in this band were mainly the 1657 Å lines of atomic carbon and the 1304 Å lines of atomic oxygen, in a ratio of peak brightnesses of 3 to 1. Comparison of the direct image and the spectrogram showed that these two lines accounted for more than two-thirds of the total direct image density; the remainder must have been due to lines and molecular bands too weak to be identified in the spectrogram. It was not possible to determine the sizes of the images on the spectrograms, except to note that they were more diffuse than stellar images (2 arc minutes across). Since most of the direct image was due to carbon emission, we used the size of that image to determine a total luminosity in the carbon lines of 1.2×10^{29} photon sec^{-1}. This is in reasonable agreement with the total luminosity observed with a spectrometer on 5 January, as described by Feldman *et al.* in the accompanying report (*2*), in view of calibration uncertainties (factors of 1.5) and the differences in distance from the sun. If the region emitting atomic oxygen is taken to be the same size as the carbon region, the resulting total luminosity is much less than observed by Feldman *et al.* with their spectrometer. A plausible explanation is that the oxygen region was much larger than the carbon region (perhaps 10^6 km across). This is to be expected since the ionization potential of oxygen

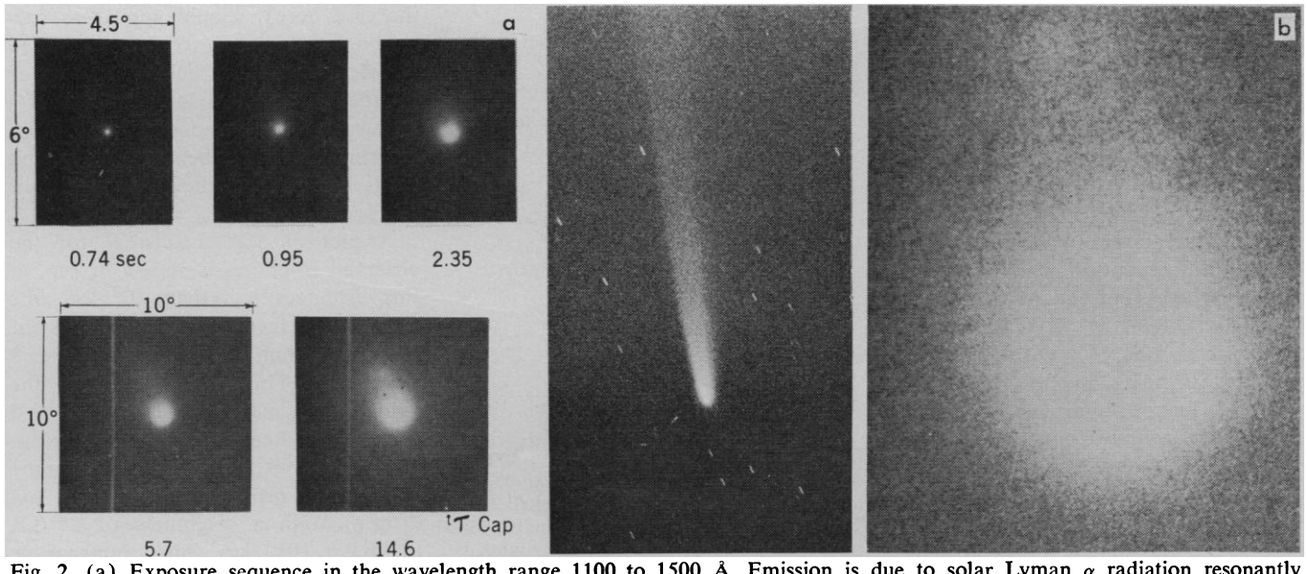

Fig. 2. (a) Exposure sequence in the wavelength range 1100 to 1500 Å. Emission is due to solar Lyman α radiation resonantly scattered by atomic hydrogen escaping from the comet. The longest exposure shows the halo out to 10^7 km from the comet. (b) The photograph at the left is a visible light image of Kohoutek on 5.1 January 1974 taken from Aerobee rocket 26.023 with an $f/2.8$, 180-mm Nikon camera. The exposure was 7 seconds on Tri-X film; development was pushed to 1200 ASA. At the right is a Lyman α image to the same scale taken with an $f/1$ electronographic Schmidt camera on 8.1 January from Aerobee 26.022.

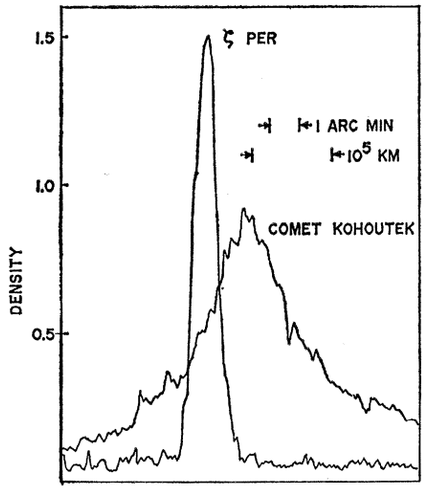

Fig. 3. Densitometer scans through the images of the comet and the star Zeta Persei (ζ Per). The central region of the comet is definitely not point-like, probably because it is optically thick to Lyman α radiation.

is higher than that of carbon, and thus the oxygen would have more time to flow outward before being ionized by extreme ultraviolet solar radiation. The relation of the observed luminosities to the production rates of these atoms depends on the product of the excitation rates (including cascading effects) and lifetimes before loss. Unfortunately, the relevant cross sections and solar spectrum are not well known. Although the sun has strong emission lines in the 1304- and 1657-Å multiplets, because of the large radial velocity of the comet these lines are Doppler-shifted out of the absorption peaks of the atoms in the comet. The matter is discussed in greater detail in the accompanying report (*2*).

The short-wavelength camera (1100 to 1500 Å) recorded emissions out to distances greater than 10^7 km from the center of the comet (Figs. 2 and 3). The shortest exposures (0.75 second) revealed a diffuse central region having a peak brightness of about 120 kiloRayleighs (kR; 1 R = $10^6/4\pi$ photon cm^{-2} sec^{-1} ster^{-1}). A similar halo, identified as being due to the 1216-Å resonance line of atomic hydrogen, was discovered around Comet Tago-Sato-Kosaka with the scanning objective spectrometer on the Orbiting Astronomical Observatory OAO-2 in January 1970 (*3*). Later that year similar emissions around Comet Bennett were traced out by the instruments on OAO-2 and the Orbiting Geophysical Observatory OGO-5. Analysis of these observations (*4*, *5*) showed that the emission was due to resonant scattering of solar Lyman α by atomic hydrogen evaporating from the comet. The great extent of the halo is due to the high velocity of the hydrogen, a consequence of its small mass and the negligible gravity of the comet. The solar Lyman α line is so wide that Doppler shifts are not very important. The source of the hydrogen is probably photodissociation of parent molecules such as H_2O.

The shape of the hydrogen cloud depends on a number of factors: the velocity distribution of the outgoing atoms, the effects of radiation pressure, the rates of loss due to ionization, the time dependence of the evaporation rate, and so on. Nevertheless, it is possible to estimate the mean outflow velocity and production rate by comparing the observed brightness contours with a simple first-order theory. We ignore loss mechanisms, optical depth effects, time dependences, and (for the time being) radiation pressure, and we assume that the hydrogen leaves a negligibly small volume near the nucleus isotropically at a rate Q atom sec^{-1} ster^{-1} and mean velocity $\bar{v}$. The density n at a distance r from the nucleus is then

$$n(r) = \frac{Q}{r^2\bar{v}} \qquad (1)$$

Each atom will resonantly scatter solar Lyman α photons at a rate g photon sec^{-1}. The observed brightness along a path with minimum perpendicular distance R to the nucleus of the comet is given by

$$B(R) = 10^{-9}gN(R) \qquad (2)$$

where the factor 10^{-9} converts the units to kiloRayleighs; N, the number

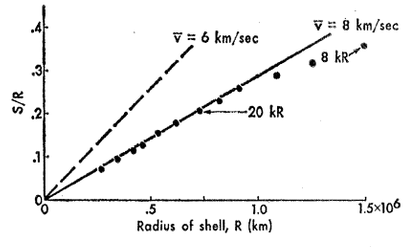

Fig. 4. Relative displacement of Lyman α shells of constant brightness (S/R) plotted against the radius of the shell (R). The brightness of two of the shells, corrected for 7 kR of airglow background, is indicated. The solid line is the displacement that would be expected to be caused by solar radiation pressure if all the escaping hydrogen atoms had the velocity $\bar{v}$ = 8 km sec^{-1}.

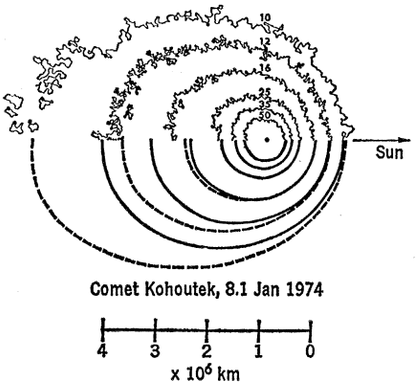

Fig. 5. Upper curves are microdensitometer tracings of the Lyman α image of Comet Kohoutek, converted to absolute intensity units. Lower curves are model isophotes for a 5.3-day lifetime (solid lines) and an infinite lifetime (dashed lines). An airglow background of 7 kR has been added to the model.

of atoms per square centimeter column, is given by the integral of $n(r)$ along the perpendicular path

$$N(R) = \frac{\pi Q}{R\bar{v}} \qquad (3)$$

In order to determine the mean velocity, we use the following considerations. A shell of atoms emitted t seconds ago will have a radius $R = \bar{v}t$. Within this first-order approximation, the center of this shell will be displaced a distance $S = \frac{1}{2}at^2 = \frac{1}{2}aR^2/\bar{v}^2$ away from the sun because of solar radiation pressure exerting an acceleration a on the atoms. Thus, Lyman α isophotes of the comet, if viewed at 90° (as was the case here), should appear as successive circles with centers displaced farther and farther behind the center of the comet (as long as $S \ll R$). At larger distances, one is really looking through a number of overlapping shells and the situation is more complicated.

A plot of S/R against R for the observed isophotes is shown in Fig. 4. For distances less than 10^6 km, the data fit perfectly the predictions of the simple outflow model with $\bar{v} = 8$ km sec^{-1}. This is the same as the value of the mean velocity determined for Comet Bennett (*4*, *5*). We can now use Eqs. 2 and 3 to determine the rate of production of atomic hydrogen. With a brightness of 25 kR at 6.2×10^5 km and appropriate values of other parameters (g = 0.0112 photon sec^{-1} atom^{-1}, $a = 3.7 \times 10^{-5}$ km sec^{-2}), we find a production rate Q of 3.6×10^{28} atom sec^{-1} ster^{-1}.

In order to match the observations at large distances from the nucleus, we have, in the next order of model improvement, followed Bertaux *et al.* (*5*). In this scheme, the atoms again flow outward from a point source, but with a thermal dispersion about the radial velocity. Charge exchange with solar wind protons is included as the principal loss process. Figure 5 shows the results computed with this model for a mean velocity of 8 km sec^{-1} and the values of g and a given above. The effect of radiation pressure is to produce elliptical, rather than circular, outer isophotes. Theoretical contours are shown for infinite and 5.3-day lifetimes to demonstrate the effects of the loss mechanism. The best fit was for the infinite lifetime case, rather than the 5.3-day lifetime which fit the Bennett data. The longer lifetime is probably due to differences in solar wind intensity. Part of the effect may also be due to a high-velocity component in the velocity distribution of the escaping hydrogen. The production rate derived from this model was 3.6×10^{28} atom sec^{-1} $ster^{-1}$, the same as that derived from the first-order theory.

For comparison, a production rate derived from the OGO-5 data on Comet Bennett was about 6×10^{28} atom sec^{-1} $ster^{-1}$ when the comet was 0.8 A.U. from the sun (*4*, *5*). If one assumes an inverse square law dependence of production rate on sun-comet distance, then the production rate for Bennett at the sun-comet distance of these observations was some six times greater than the production rate for Kohoutek.

C. B. Opal
G. R. Carruthers
D. K. Prinz
R. R. Meier

U.S. Naval Research Laboratory, Washington, D.C. 20375

References and Notes

1. G. R. Carruthers and T. L. Page, *Science* **177**, 788 (1972); G. R. Carruthers, *Appl. Opt.* **12**, 2501 (1973).
2. P. D. Feldman, P. Z. Takacs, W. G. Fastie, B. Donn, *Science* **185**, 705 (1974).
3. A. D. Code, T. E. Houck, C. F. Lillie, *NASA SP-310* (1972), p. 109.
4. H. U. Keller, *Astron. Astrophys.* **27**, 51 (1973).
5. J. L. Bertaux, J. E. Blamont, M. Festou, *ibid.* **25**, 415 (1973).
6. We are grateful to the Sounding Rocket Division of the National Aeronautics and Space Administration for supplying and providing field support for the rocket. The Air Force Avionics Laboratory provided much of the funding to build the payload. We thank U. Keller and P. Feldman for helpful discussions. H. Merchant and D. King assisted in the preparation of the payload.

22 April 1974

Rocket Ultraviolet Spectrophotometry of Comet Kohoutek (1973f)

Abstract. *Observations of Comet Kohoutek (1973f) in the spectral region between 1200 and 3200 angstroms were made from an Aerobee rocket on 5.1 January 1974 universal time. The strongest features observed were the Lyman alpha line of neutral atomic hydrogen at 1216 angstroms and the hydroxyl (OH) bands at 3090 and 3142 angstroms. Atomic oxygen and atomic carbon were also detected, and their luminosity implies a production rate (of carbon monoxide or carbon dioxide) commensurate with that of water vapor.*

An Aerobee 200 rocket carrying two spectrophotometers was launched from White Sands Missile Range (New Mexico) at 0145 U.T. on 5 January 1974 to study the ultraviolet emissions from Comet Kohoutek (1973f) in the spectral range 1200 to 3200 Å. At the time of launch, the comet-sun-earth angle was 20.3° and the sun was 5° below the rocket horizon at apogee (232 km). Scattered sunlight near the horizon made it difficult for the star tracker of the attitude control system to lock on the comet, whose magnitude was estimated visually at $m_v \approx +2.5$, approximately three magnitudes weaker than predicted. Nevertheless, several seconds of data on the coma were obtained, and observations of the tail were obtained during rocket descent after the star tracker locked on when the solar depression angle exceeded 7°.

In addition to the Lyman α line of atomic hydrogen (HI) at 1216 Å and the (0, 0) and (1, 1) bands of OH at 3090 and 3142 Å, which were previously observed in Comet Bennett (1970 II) by the Orbiting Astronomical Observatory OAO-2 (*1*), both atomic oxygen (OI) (1304 Å) and atomic carbon (CI) (1657 and 1561 Å) were detected; the derived luminosities are commensurate with those observed by Opal *et al.* (*2*) 3 days later. No other spectral features are clearly identified, from either the coma or the tail.

The payload consisted of two scanning Ebert spectrophotometers, each with an off-axis paraboloid of 50-cm focal length which focused the image of the comet on the entrance slit. One spectrometer, with a focal length of 25 cm, covered the wavelength range from 1200 to 1700 Å at a resolution of 10 Å with an effective field of view of 7 by 35 arc minutes. The other, with a 12.5-cm focal length, monitored the spectral region from 1800 to 3200 Å at a resolution of 15 Å with a field of view of 3.5 by 21 arc minutes. In both cases, the long axis of the slit was oriented perpendicular to the sun-comet line. A CaF_2 filter was used to reduce the sensitivity of the short-wavelength spectrometer at 1216 Å by a factor of ≈ 100 in order to prevent instrumental scattering of the strong Lyman α signal from masking spectral features at the limit of detectability. A Nikon F camera with a programmed motor drive and a lens with a focal length of 180 mm was included for aspect information.

Spectral data are shown in Fig. 1. The short-wavelength spectrum is shown on an expanded vertical scale and is the sum of all the data obtained with

Table 1. Ultraviolet emissions from Comet Kohoutek (1973f). Abbreviations: λ, wavelength; F, flux; L, luminosity; g, emission rate factor (at 1 A.U.); τ, lifetime (at 1 A.U.); and Q, production rate.

Species	λ (Å)	F (photon sec^{-1} cm^{-2})	L (photon sec^{-1})	g (photon sec^{-1} mol^{-1})	τ (sec)	Q (sec^{-1})
OI	1304	120 ± 40	2.8×10^{29}	5.0×10^{-7}*	4.0×10^{6}	1.4×10^{29}
CI	1657	140 ± 50	3.3×10^{29}	1.1×10^{-5}*	2.5×10^{6}	1.2×10^{29}
OH	3090	3100 ± 100	7.4×10^{30}	1.2×10^{-3}*	7.9×10^{4}	0.8×10^{29}
CO	1510	≤ 15	$\leq 4 \times 10^{28}$	8.2×10^{-5}	6.9×10^{5}	$\leq 7.1 \times 10^{29}$
CO_2	2890	≤ 18	$\leq 4 \times 10^{28}$	9.1×10^{-5}	3.9×10^{5}	$\leq 1.1 \times 10^{30}$
HI	1216			2.1×10^{-3}		5.4×10^{29}
				5.2×10^{-3}†		2.2×10^{29}†

* A Doppler shift of 55 km sec^{-1} was allowed for. † Derived by using the solar Lyman α flux of Keller and Thomas (*11*).